Eur Biophys J (2001) 30: 344–353
DOI 10.1007/s002490100151

ARTICLE

Erkut İnan İseri · Demet Gülen

Chlorophyll transition dipole moment orientations and pathways for flow of excitation energy among the chlorophylls of the major plant antenna, LHCII

Received: 25 July 2000 / Revised version: 27 February 2001 / Accepted: 1 March 2001 / Published online: 3 May 2001

Abstract We have attempted in this work an assignment of the Q_y dipole moment orientations for all the chlorophylls in the major plant antenna, light-harvesting complex II (LHCII). Information that has recently become available through a structural model of the LHCII, site-directed mutagenesis, and spectroscopy of both LHCII and CP29 has been evaluated to model the electronic excited state structure in the presence of chlorophyll-chlorophyll and chlorophyll-protein interactions. An assignment has been obtained which satisfactorily reproduces the polarized linear absorption characteristics. The assignment proposed has also been found to be adequate in reproducing the time scales of the energy transfer processes. The pathways for the flow of excitation energy among the chlorophylls of the complex have been suggested in the context of identity and orientation assignments.

Keywords Light-harvesting complex II · Electronic excited states · Energy transfer · Photosynthesis

Abbreviations *ABS*: absorption · *CD*: circular dichroism · *Chl*: chlorophyll · *LD*: linear dichroism · *LHC*: light-harvesting complex · *PSII*: photosystem II · *3PEPS*: three-pulse photon echo peak shift

Introduction

Photosynthetic organisms contain light-harvesting pigment-protein complexes (LHCs) that absorb light and transfer energy efficiently to other pigment-protein complexes called reaction centers to initiate the photochemistry of photosynthesis. The efficiency of the light-harvesting processes depends on the ultrafast energy transfer processes in the LHCs (antenna) of green plants, bacteria, and algae, which are mainly governed by the pigment-pigment and the pigment-protein interactions. For a comprehensive understanding of the ultrafast energy transfer processes on the molecular level, one of the important tasks is the determination of the electronic excited states of the LHCs (van Grondelle et al. 1994).

Light-harvesting in photosystem II (PSII) of green plants is performed by a collection of LHCs buried in the photosynthetic membrane (thylakoids). The LHC associated with the PSII consists of two parts: an outer antenna binding chlorophyll *a* (Chl *a*), Chl *b*, and carotenoids as pigments and an inner antenna binding Chl *a* and carotenoids. The proteins forming the outer antenna are usually called as the Lhcb proteins. The major Lhcb protein, LHCII, binds almost 65% of the PSII chlorophyll (accounting for 50% of the total Chls in the thylakoids), and three of the minor Lhcb proteins homologous to LHCII (usually called as CP24, CP26, and CP29) bind altogether 15% of the PSII chlorophyll (Boekema et al. 1999).

Currently, LHCII is the only Lhcb protein which is structurally resolved. A large part of the structure of the LHCII is modeled to a resolution of 3.4 Å (Kühlbrandt et al. 1994). The LHCII pigments identified per monomeric subunit of the C_3 symmetric trimer of the current model are 12 Chl molecules surrounding two central carotenoid molecules (see Fig. 1).

The current LHCII model does not allow a direct access to several parameters that are essential for understanding the light-harvesting function. At 3.4 Å resolution the Chls could only be modeled as naked tetrapyrrole rings. Therefore, the model does not provide any distinction between the Chls *a* and *b* (the identity problem) and no distinction could be made between the molecular *x*- and *y*-axes of the Chl molecules (the orientation problem).

However, most of the chlorophyll binding sites in LHCII are disclosed by the structural model, which also

E.İ. İseri · D. Gülen (✉)
Department of Physics, Middle East Technical University,
06531 Ankara, Turkey
E-mail: dgul@metu.edu.tr
Fax: +90-312-2101281

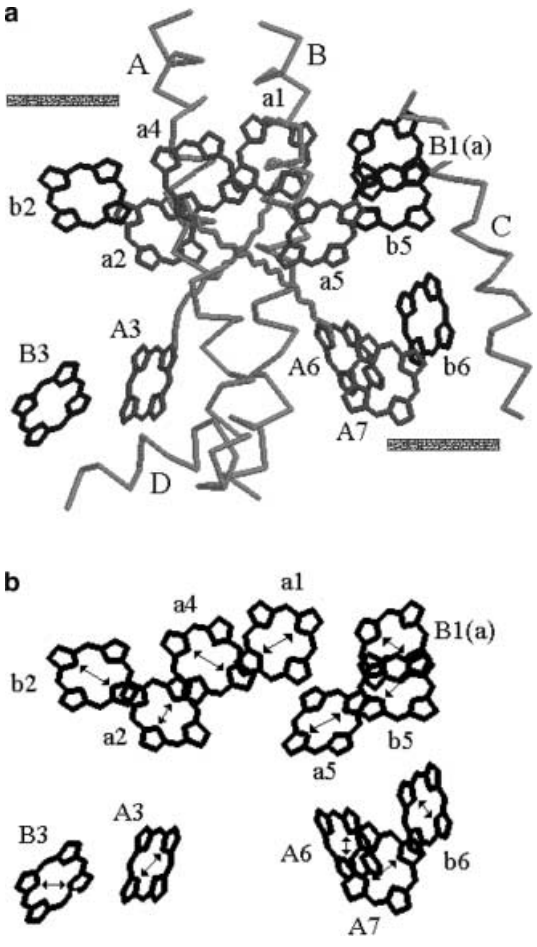

Fig. 1 **a** A 2-D view of the LHCII structure. The protein folding of LHCII consists of three membrane-spanning α-helices (*A*, *B*, and *C*) and a fourth helix (*D*) running parallel to the presumed position of the photosynthetic membrane. The helices *A* and *B* are related to each other by a two-fold symmetry axis running perpendicular to the membrane (parallel to the C_3 symmetry axis). The 12 chlorophyll (Chl) molecules surround the two central carotenoids. In our model, a1, a2, a4, and a5 are Chl *a* molecules; b2, b5, and b6 are Chl *b* molecules. The mixed sites, A3, B3, A6, and A7, bind Chl *a* and Chl *b* with equal affinities. **b** The protein and the carotenoids are stripped off for clarity. The *diagonal arrows* on the tetrapyrrole rings of the Chls indicate approximately the directions of the Q_y transition dipoles determined in this study

led to the identification of the probable binding sites in highly homologous CP29 (Bassi et al. 1999). Site-directed mutagenesis of chlorophyll binding residues has allowed construction of several mutant proteins lacking individual Chl molecules. Biochemical and spectral characterization of these mutants has recently been used for determination of the Chl identities in both CP29 and LHCII (Bassi et al. 1999; Remelli et al. 1999; Rogl and Kühlbrandt 1999; Simonetto et al. 1999). Bassi and co-workers have reported that in both complexes the evolutionarily conserved core (Green and Kühlbrandt 1995), consisting of the binding sites A1, A2, A4, and A5, is found to be occupied by the Chls *a*. In CP29 the remaining four binding sites (A3, B3, B5, and B6) are found to have mixed Chl *a*/*b* occupancies, with the respective Chl *a* binding probabilities of 70%, 30%, 60%, and 40%. However, in reconstituted monomeric LHCII, A3 and B3 are found to be mixed sites with equal Chl *a*/*b* binding affinities and B5 and B6 are found to be pure Chl *b* sites. Three of the remaining LHCII sites are suggested to bind either Chl *b* (A7 and B2) or Chl *a* (B1), and A6 is proposed to have equal affinity for Chl *a* and *b*. On the other hand, Rogl and Kühlbrandt (1999) have suggested that A1, A2, A3, and B3 are pure Chl *a* sites and B5 and B6 are pure Chl *b* sites in reconstituted trimers.

There is no doubt that determination of the Chl identities is a major step in correlating the spectra with the structure. However, understanding of the structure-function relationship is still hampered since the orientations of the molecular *y*-axis of the Chls are not unambiguously determined.

The Lhcb proteins are spectroscopically complex objects, exhibiting considerably heterogeneous spectra in the spectral range of 630–685 nm (Q_y band) and many spectral forms are commonly observed in all the Lhcb proteins in this absorption region. The number of spectral bands decomposed in the Q_y band almost matches the number of bound Chls in all these complexes (Zucchelli et al. 1994). Owing to a fewer number of Chls, the minor antennae show a lower degree of complexity and their spectral data may prove more easily interpretable than that of the LHCII. It has long been noted that the spectral bands resolved in the Chl *a* absorption region of the LHCII and CP29 proteins are essentially identical, suggesting an identical organization for the Chls *a* common to both complexes (Zucchelli et al. 1994; Giuffra et al. 1997). In the recent site-directed mutagenesis work of Remelli et al. (1999), it has been furthermore confirmed that not only the site selectivity is largely conserved between the two complexes but also the distribution of the absorption forms among different protein domains. In addition, the energy equilibration in CP29 is observed to be very similar to part of the energy equilibration in LHCII, both in terms of temporal and spectral characteristics (Gradinaru et al. 1999). It has therefore been expected that a better interpretation of the light-harvesting process in the major plant antenna, LHCII, can be obtained by understanding the structurally and electronically less complicated CP29.

Recently, we have suggested an electronic excited state structure for the CP29 complex (seri et al. 2001) by assuming a structure common with the relevant part of the LHCII and using the Chl identities reported by the mutational analysis of Bassi et al. (1999). We have determined the orientations of the Q_y transition dipole moments of all the Chls of CP29 by a simultaneous simulation of the key features of the low-temperature absorption (ABS) and linear dichroism (LD) spectra (Pascal et al. 1999). We have also discussed that the model we proposed can explain the general character of the energy equilibration in CP29 (Gradinaru et al. 1999) on the basis of our preliminary energy transfer rate estimates.

In the present study we have attempted to assign the orientations of all the LHCII chlorophylls using our

recent orientational assignments for the CP29 Chls and most of the identities of the LHCII Chls recently reported (Remelli et al. 1999). We have evaluated a considerable part of the extensive spectroscopic data on the Chl excited states and Chl interactions in LHCII (Eads et al. 1989; Hemelrijk et al. 1992; Krawzcyk et al. 1992; Kwa et al. 1992; van Amerongen et al. 1994; Bittner et al. 1994; Du et al. 1994; Nussberger et al. 1994; Palsson et al. 1994; Reddy et al. 1994; Savikhin et al. 1994; Lokstein et al. 1996; Visser et al. 1996; Connelly et al. 1997; Kleima et al. 1997; Gradinaru et al. 1998; Agarwal et al. 2000) in the presence of both the coulombic interactions between the Chls and the pigment-protein interactions. We have suggested an assignment which satisfactorily reproduces the key features of the polarized linear absorption characteristics as well as the prominent spectral and temporal features of the energy transfer processes among the chlorophylls.

Table 1 The 16 LHCII configurations

Configuration	A3	A6	A7	B3
1	*a*	*a*	*a*	*a*
2	*a*	*a*	*b*	*a*
3	*a*	*b*	*a*	*a*
4	*a*	*b*	*b*	*a*
5	*b*	*a*	*a*	*a*
6	*b*	*a*	*b*	*a*
7	*b*	*b*	*a*	*a*
8	*b*	*b*	*b*	*a*
9	*a*	*a*	*a*	*b*
10	*a*	*a*	*b*	*b*
11	*a*	*b*	*a*	*b*
12	*a*	*b*	*b*	*b*
13	*b*	*a*	*a*	*b*
14	*b*	*a*	*b*	*b*
15	*b*	*b*	*a*	*b*
16	*b*	*b*	*b*	*b*

Materials and methods

Coulombic interaction between the pairs of Chls is assumed to be the relevant physical mechanism and the interactions between the Chls are treated in the point dipole approximation. Pigment-protein interactions (Simonetto et al. 1999; İseri et al. 2001) are only described through a wavelength shift of the Chl site energies (the transition energies in the protein environment in the absence of pigment-pigment interactions). The spectra (ABS and LD) are simulated using the exciton formalism (Pearlstein 1991), as we have described elsewhere in detail (İseri 1998).

The information needed to simulate the experimental spectra at the level of approximation we have used involves:

1. Identities of the Chl molecules as *a* and *b*.
2. Distances between the Chl molecules.
3. Effective absorption strengths of the Chls in the protein environment corresponding to the Q_y band (0-0) transitions.
4. Orientations of the individual Q_y transition dipole moments for the Chl *a* and Chl *b* molecules.
5. Site energies of the Chl molecules.

The LHCII structural model is used for the organization of the Chls in the LHCII (see Fig. 1a). The calculations are restricted to a monomeric unit of the C_3 symmetric LHCII trimer. The atomic coordinates of the tetrapyrrole rings of the LHCII complex are used to determine the distances between the Chls and the two possible directions of the molecular *y*-axis for each of the 12 Chls.

Except for the identity of the molecule binding to site A7, the Chl identities recently determined by Remelli et al. (1999) are used: a1, a2, a4, a5, and B1(*a*) are Chl *a* molecules; b2, b5, and b6 are Chl *b* molecules; and A3, B3, and A6 are mixed sites. In this mutagenesis study, A7 is suggested to be a pure Chl *b* site. However, for reasons discussed below we have assigned this site also as a mixed one. We have assumed equal *a* and *b* binding probabilities for A7 for the sake of simplicity. Owing to presence of four mixed sites there are 16 different configurations for the 12 Chls of the LHCII complex. Since all the mixed sites have/are assumed to have equal (50%) Chl *a* and Chl *b* occupancies, all 16 configurations given in Table 1 have equal probability of occurrence (6.25%).

The effective absorption strength corresponding to the Q_y (0-0) transitions of each Chl *a* is taken as $\mu_a^2 = 20\ D^2$, following the recent determination by Kleima et al. (2000) for the monomeric Chl *a* in the protein environment of *Amphidinium carterae* (Hofmann et al. 1996). The effective absorption strength for each Chl *b* is taken as $\mu_b^2 = 14\ D^2$ by keeping $\mu_b^2/\mu_a^2 = 0.7$ (Sauer et al. 1966). This effective value is estimated to correspond to a refractive index of 1.6 ± 0.1 (Kleima et al. 2000). The remaining parameters (the site energies in the Q_y band and the direction of the molecular *y*-axis for each Chl) have been determined through a satisfactory simultaneous simulation of the key features of the ABS and LD spectra.

The nomenclature of Gülen et al. (1995, 1997) for the two possible directions of the molecular *y*-axis, i.e. 0 (along the N_A-N_C axis) and 1 (along the N_B-N_D axis) is maintained. Here the subscripts refer to the convention of the file provided by Dr. Werner Kühlbrandt.

The orientations of the Chls a1 (0), a2 (1), A3 (0), a4 (0), a5 (0), B3 (1), b5 (1), and b6 (0) are fixed using our results on the CP29 chlorophylls. The Q_y transition dipole moment direction of each Chl *a* molecule is assigned along the molecular *y*-axis (i.e. 0 or 1), while those of the Chl *b* molecules are rotated by ± 5–$10°$ from the molecular *y*-axis (see the Discussion below). The sense of the rotations, "+/–", are defined as the clockwise/counter-clockwise rotations of the vectors from N_D to N_B and from N_A to N_C, where the nitrogens are viewed counter-clockwise from N_A to N_D.

The LD analysis is performed in the convention of Simonetto et al. (1999). The C_3 symmetry axis of the trimeric LHCII (or the pseudo-two-fold internal symmetry axis of the LHCII monomers) is defined as a normal to "the molecular plane", which is the plane in which the membrane presumably lies (see Fig. 1a). It is assumed that the macroscopic alignment axis of the LD measurements is parallel to the molecular plane (i.e. perpendicular to the C_3 symmetry axis) and $LD = A_{||} - A_{\perp}$ where $A_{||(\perp)}$ is the absorption parallel (perpendicular) to the macroscopic alignment axis.

The spectra are simulated as weighted sums of the gaussian dressed spectrum of each of the 16 configurations. Each excitonic transition in the Q_y region is dressed by a symmetric gaussian of bandwidth 8 nm.

We have compared the simulations with the low-temperature ABS and LD data for the trimeric LHCII (van Amerongen et al. 1994), in the absence of low-temperature spectra of the reconstituted monomeric LHCII. The ABS spectrum of the reconstituted monomeric LHCII at room temperature is almost identical to that of the native trimeric LHCII (Remelli et al. 1999). Although there exist low-temperature data for several monomeric LHCII prepared by other techniques (Nussberger et al. 1994), we have avoided comparing with these as the samples are likely to have Chl *a*/*b* binding properties not identical to that of the reconstituted monomeric LHCII.

Results

The aim has been to propose the orientations and the site energies of all 12 chlorophylls of an LHCII monomer by

a simultaneous simulation of the ABS and LD spectra. Having fixed the Q_y dipole moment directions of eight of the Chls common to both CP29 and LHCII, there remain four Chl dipole moment directions to be determined. Since for each Chl there are two possible orientations for the molecular *y*-axis, there are $2^4 = 16$ possible dipole moment conformations to be judged.

We have tested each of these 16 dipole moment conformations to determine the best solution. Although we have not provided any simultaneous fits, we have also inspected whether a selected conformation can account for the general character of the *b*-*b*, *b*-*a*, and *a*-*a* excitation transfer kinetics. We have not attempted to fit the circular dichroism (CD) spectrum since it is very sensitive to minor changes in the orientations of the Chls. Furthermore, the experimental CD spectrum at room temperature (and also at low temperature) is not conservative; especially, the origin of the large, nonconservative, negative CD signal in the Chl *b* absorption region is unknown. Such a signal is also present in CP29, LHCII, CP26, and reconstituted complexes with varying Chl *a*/*b* ratios (see e.g. Kleima et al. 1999). In our calculations, one would obtain a conservative CD spectrum by definition.

Under the assumption that the mixed sites bind Chls *a* and *b* in the same geometry, the best solution we have found has the following parameters: orientational assignments: a1 (0), a2 (1), a4 (0), a5 (0), B1(*a*) (0), b2 (0), b5 (1), b6 (0), A3 (0), B3 (1), A6 (1), and A7 (0) (see Fig. 1b); site energies (in nm): a1 (668), a2 (672), a4 (674), a5 (674), B1(*a*) (667), A3 (*a*, 672), B3 (*a*, 665), A6 (*a*, 673), A7 (*a*, 667), b2 (645), b5 (647.5), b6 (649.5), A3 (*b*, 653), B3 (*b*, 651), A6 (*b*, 653), and A7 (*b*, 649). Note that we have not fixed the site energies of the Chls common to the LHCII and CP29 complexes. Although most of the sites present in both complexes induce similar absorption characteristics, some sizable differences have been observed in several binding sites (e.g. A3, B3, and a2), possibly owing to different pigment-protein interactions (Remelli et al. 1999).

To have a satisfactory fit of the Chl *b* region LD properties, it has been necessary to allow around ± 5–$10°$ deviations from the molecular *y*-axis for the Chl *b* dipole moments and this has also been the case in the CP29 simulations. The rotations have been b2 (–10°), b5 (–10°), b6 (10°), A3 (–10°), B3 (10°), A6 (5°), and A7 (10°). The effect of rotations on the interaction matrix elements is negligible.

In Fig. 2 the ABS and LD spectra have been presented for the solution given above and have been compared with the LHCII experimental data (van Amerongen et al. 1994). Each of the simulated spectra is the weighted average of the gaussian dressed spectrum for each of the 16 LHCII configurations.

We would like to note that we have only considered the 0-0 transitions and have made no attempt to introduce the phonon wing/vibrational transitions. The Chl *a* wing contributes significantly around 660 nm for a Chl *a* 0-0 transition around 675 nm. We attribute the differences between the simulated and measured ABS spectra and the inconsistencies in the LD spectra around 662 nm to the neglect of phonon wing/vibrational transitions. An absorption offset between 630 and 660 nm is also present in the ABS simulations of CP29 (Simonetto et al. 1998; İseri et al. 2001) and is attributed similarly to the neglect of the vibrational tails in the Chl *a* absorption forms.

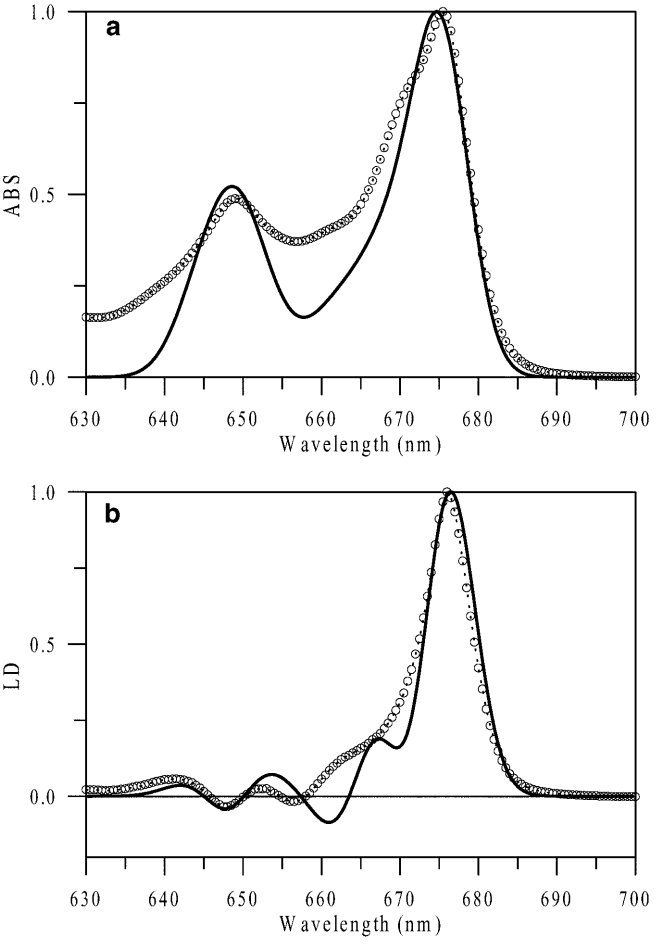

Fig. 2 Experimental spectra (*open circles*) versus simulations (*solid lines*): **a** ABS; **b** LD. Experimental data at 77 K are reproduced from van Amerongen et al. (1994)

The transitions which occur in the 16 different LHCII configurations can be classified in terms of their delocalization characteristics. The classifications for the "Chl *a*" (660–677 nm) and the "Chl *b*" (645–656 nm) spectral regions are given, respectively, in Tables 2 and 3. The electronic excited state structure in the "Chl *a*" spectral region is decided to a large extent by the interactions within the following groups of Chls *a*: a1-a2-B1(*a*) (a1-a2$\approx$–65 cm^{-1} and a1-B1(*a*) $\approx$100 cm^{-1}), a4-a5 ($\approx$45 cm^{-1}), B3(*a*)-A3(*a*) ($\approx$–155 cm^{-1}). There are also several weaker cross-couplings between these three groups which cause further delocalization of excitation. The pairs a4-a5 and A3-B3 are cross-coupled through the interactions of A3 with both a4 and a5 ($\approx$–10 and $\approx$–20 cm^{-1}, respectively). The a1-a2-B1(*a*) triplet is cross-coupled with the a4-a5

Table 2 Properties of the "Chl *a*" region (660–677 nm) transitions

	Wavelength (nm)	ABS strength (D^2)	Composition[a]	Configurations
I	660.7	19	A3(*a*), B3(*a*) (28, 72)	1, 2, 3, 4
II	662.6	12	a1, B1 (47, 49)	All
IIIa	666.7	6	A3(*b*), B3(*a*) (10, 80)	5, 6
IIIb	666.8	18	A3(*b*), B3(*a*) (11, 87)	7, 8
IVa	667.7	35	A7(*a*), b6 (88, 5)	1, 3, 9, 11, 13, 15
IVb	667.9	50	A7(*a*), B3(*a*), b6 (81, 7, 5)	5, 7
V	670	8	a1, a2, B1 (23, 35, 40)	All
VIa	671.5	6	A3(*a*), a4, a5 (22, 34, 37)	9, 10, 11, 12
VIb	671.9	7	a4, a5 (45, 45)	1, 2, 3, 4
VIc	672	9	a4, a5 (49, 45)	5, 6, 7, 8
VId	672.1	11	a4, a5 (50, 47)	13, 14, 15, 16
VIIa	673.7	31	A3(*a*), a4, A6(*a*) (54, 20, 13)	9, 10
VIIb	673.8	18	A3(*a*), a4 (71, 20)	11, 12
VIIc	674	21	A6(*a*) (92)	1, 2, 5, 6, 13, 14
VIId	674.1	6	A3(*a*), A6(*a*) (17, 75)	9, 10
VIIIa	675	35	a1, a2, a4, b1 (23, 46, 12, 10)	1, 2, 3, 4
VIIIb	675.1	54	a1, a2, a4, b1 (26, 50, 7, 11)	Others
IXa	676.2	8.5	a1 + a2, a4, a5 (15, 40, 37)	1, 2, 3, 4
IXb	676.3	15	a1 + a2, a4, a5 (10, 42, 47)	5, 6, 7, 8, 13, 14, 15, 16
IXc	676.3	18	a1 + a2, a4, a5 (10, 40, 49)	9, 10, 11, 12
X	676.8	45	A3(*a*), a5, B3(*a*) (62, 12, 23)	1, 2, 3, 4

[a]The molecules contributing and the respective percentage contribution (in parentheses). The numbers in the first three columns are the values averaged over the configurations given in the last column

Table 3 Properties of the "Chl *b*" (644–656 nm) region transitions

	Wavelength (nm)	ABS strength (D^2)	Composition[a]	Configurations
Ia	644	6	A7(*b*), b2, b5, b6 (16, 40, 10, 25)	4, 8, 12, 16
Ib	644.1	12	b2 (93–95)	Others
IIa	644.3	11	A7(*b*), b2, b6 (16, 56, 17)	4, 8, 12, 16
IIb	644.8	2	A7(*b*), b5, b6 (38, 16, 38)	2, 6, 10, 14
IIc	645	11	A6(*b*), b5, b6 (15, 30, 45)	3, 7, 11, 15
IId	645.9	7.5	b5, b6 (50, 44)	1, 5, 9, 16
IIIa	647.7	17–20	A7(*b*), b5 (23, 75)	2, 4, 6, 8, 10, 12, 16
IIIb	647.8	14	A7(*b*), b5 (22, 65)	14
IV	648.1	20	A3(*b*), B3(*b*) (35, 65)	13, 14, 15, 16
Va	648.7	27	b5, b6 (67, 23)	3, 7, 11, 15
Vb	649.2	23	b5, b6 (47, 49)	1, 5, 9, 13
VI	649.8	12–20	A3(*a*), B3(*b*) (5, 93)	9, 10, 11, 12
VIIa	650.4	38	A3(*b*), A6(*b*), A7(*b*), b5, b6 (13, 21, 35, 10, 20)	8
VIIb	650.5	28	A6(*b*), A7(*b*), b5, b6 (24, 42, 10, 24)	4, 12, 16
VIIIa	651	13	A3(*b*), B3(*a*) (88, 12)	5, 7
VIIIb	651.1	26	A3(*b*), B3(*a*) (77, 10)	6
VIIIc	651.1	7	A3(*b*), B3(*a*) (75, 11)	8
IXa	651.3	29	A3(*b*), A7(*b*), b6 (15, 40, 37)	2, 10
IXb	651.8	18	A3(*b*), A7(*b*), b6 (15, 31, 46)	6
IXc	652	26	A7(*b*), b6 (45, 47)	14
Xa	655.5	4	A6(*b*), b6 (73, 24)	3, 7, 11, 15
Xb	655.6	7	A6(*b*), b6 (64, 33)	4, 8, 12, 16
XIa	655.9	13	A3(*b*), B3(*b*) (62, 37)	13, 14, 15, 16

[a]The molecules contributing and the respective percentage contribution (in parentheses). The numbers in the first three columns are the values averaged over the configurations given in the last column

pair via the interactions of a1 and B1 with both a4 and a5, with strengths ranging from –6 to 15 cm^{-1}. The a4-a5 pair predominantly contributes to the bands in the middle (671.5–674 nm) and in the red (675–676 nm), while the a1-a2-B1 triplet and the B3-A3 pair are associated with both the red and the blue (660–667 nm) sides of the spectrum. In addition, the strong coupling between the B3(*a*) and A3(*b*) molecules delocalizes the excitation between the two spectral regions and yields a band around 667 nm. One of the remaining two Chls *a*, A6, has the strongest interaction with A7 (≈–35 cm^{-1}) and is also weakly coupled with A3 and a4 (both ≈ –10 cm^{-1}). In addition to the A6-A7 coupling, A7 is also coupled with a5 (≈25 cm^{-1}). Moreover, both A6 and A7 are also coupled strongly with Chl b6 (A6-b6≈–105 cm^{-1} and A7-b6≈100 cm^{-1}). However, owing to their widely different site energies, A6 and A7 do not mix with each other. A6 mixes with A3 and a4 and contributes to a

band around 674 nm. A7 contributes to a blue state (≈667 nm), which is delocalized over the Chl A7 and the Chl b6 molecules. A similar *b*-*a* excitation delocalization via the equally strong b6-A6 coupling is more limited (2–3%, not shown in Table 2) owing to a larger separation in the site energies.

The Chl *b* region transitions (644–656 nm) are more congested than that of the Chl *a* region transitions. There are several important pairwise *b*-*b* interactions shaping up the spectra: A3(*b*)-B3(*b*) (≈–110 cm^{-1}), A6(*b*)-b6 (≈–90 cm^{-1}), A7(*b*)-b6 (≈85 cm^{-1}), b5-b6 (≈35 cm^{-1}), and A6(*b*)-A7(*b*) (≈–25 cm^{-1}). In particular, the coupling of b6 with A6, A7 and b5, and a further A6-A7 interaction offer a multitude of possibilities for the transitions ranging between 645 and 652 nm as shown in Table 3. In addition, the *b*-*a* couplings between B3 and A3 (≈–130 cm^{-1}) contribute to the spectra around 650–651 nm. The most uncoupled Chl *b*, b2, contributes to the blue-most transitions (≈644–645 nm) and the red-most transitions (≈656 nm) are attributed to the A3(*b*)-B3(*b*) and A6(*b*)-b6 interactions.

Discussion

The assignment of the Q_y transition dipole moment of each Chl *a* molecule along the molecular *y*-axis (i.e. 0 or 1) is based on a number of studies in which either monomeric or a pair of very weakly interacting Chl *a* molecules in a very well-defined geometry are analysed. In all these analyses the Q_y transition dipole moments of Chl *a* have been found to be almost (within about 5°) along the molecular *y*-axis. In angle-resolved fluorescence depolarization experiments on monomeric Chl *a* oriented in anhydrous nitrocellulose films, the Q_y transition dipole moment for absorption has been reported to be along the molecular *y*-axis (van Zandvoort et al. 1995). In the monomeric unit of peridinin-chlorophyll *a*-protein from *A. carterae* (a very weakly interacting pair of Chl *a* molecules in a very well-defined geometry), the Chl *a* dipole moment corresponding to the Q_y absorption has been concluded to lie very close to the molecular *y*-axis (Kleima et al. 2000). A similar result has also been reported in a dimer of very weakly interacting chlorophyllides embedded in the heme pockets of hemoglobin (Moog et al. 1984). Moreover, it has recently been possible to explain the key features of various steady-state spectra of the Fenna-Matthews-Olson protein by assigning the Q_y transition dipole direction of each of the seven bacteriochlorophyll *a* molecules along the molecular *y*-axis (Louwe et al. 1997; Vulto et al. 1998; İseri and Gülen 1999).

We are not aware of any study of the kind in which a very well-defined geometry is used for the determination of the transition dipole moment direction of the Chl *b* molecule. In the literature there have been reports suggesting a 10° difference between the Q_y dipole moment directions of the Chl *a* and the Chl *b* molecules (e.g. Fragata et al. 1988 and references therein).

The point of departure for assigning the orientations of the CP29 Chls has been the results reported in a series by Gülen et al. (1995, 1997) and by Gradinaru et al. (1998). In these series of papers the most probable orientations have been suggested upon performing a quite extensive search in a large space of possible combinations of the individual dipole moment orientations. Although this search procedure has been applied to CP29 prior to the "full" Chl identification, the model used has been very similar (in terms of structural and identity assumptions) to the one suggested in the recent work of Bassi and co-workers (1999). The combinations that can comply with the global features of both the polarized steady-state spectra and the temporal and spectral behavior of the kinetic observations have been selected. An unambiguous solution for the orientations could not be found since the selection is based on a set of relatively mild criteria, but a very restricted set of possible orientational configurations has been offered. The most probable orientational assignments for the CP29 chlorophylls (judged mostly by the polarized absorption characteristics) have been: a1 (0), a2 (0 or 1), A3 (*a*, 0 or 1), a4 (0), a5 (0), B5 (*a*, 0 or 1), B3 (*b*, 1), and B6 (*b*, 0). We have recently suggested a unique, most probable orientation set by fixing the orientations of a2 (1), A3 (0), and B5 (1) through an analysis similar to the one presented in this work (İseri et al. 2001). In Gradinaru et al. (1999), for the remaining LHCII Chls, only the orientation of A7 has been found to prefer one of the orientations (0) but it was assigned as a pure Chl *a* site. Moreover, B1, b2, and A6 are assigned as pure Chl *b* sites. We have therefore carried out our calculations with two possible orientations for each of these four Chls.

The existence/absence of several Chls *a* cause some notable differences between the delocalization characteristics of the transitions associated with the Chl *a* core common to CP29 and LHCII. These differences can be attributed mainly to the existence of B1(*a*) and the absence of B5(*a*) in the LHCII. The coupling between the a1-a2 and a4-a5 pools (mainly via a1-a5≈15 cm^{-1}) causes considerable delocalization of excitation over these four Chls *a* in the CP29. However, a much stronger B1(*a*)-a1≈100 cm^{-1} coupling in the LHCII limits the mixing between these two pairs of Chls *a*. Similarly, A3(*a*)-a5 coupling (≈–20 cm^{-1}), which leads to non-negligible delocalization of A3(*a*) with the a4-a5 pool in the LHCII, does not yield any significant delocalization in the CP29, since in this case the coupling of the a4-a5 pair with B5(*a*) overtakes. Furthermore, the delocalization between the Chl *b* and the Chl *a* pools originating from the B3-A3 interactions is more pronounced in the LHCII in these molecules as Chls *b* absorb 10 nm to the red compared to their absorption in the CP29.

The spectral complexity in the Chl *b* absorption region is almost entirely a result of the recent Chl *b* identity assignments (Remelli et al. 1999). If A3, A6, and A7 had no Chl *b* character, as in the original Kühlbrandt et al. (1994) assignment, the only important *b*-*b*

interaction would be the b5-b6 interaction and the excitation delocalization in the Chl *b* region would be much more restricted.

Remelli et al. (1999) have also assigned the transition energies of all the Chls in LHCII by comparing the spectral properties and pigment composition of LHCII with and without binding a specific Chl. It has been noted that the excitonic effects are present in the difference spectra, but the conclusions about the spectral decomposition of the Q_y band have been mainly drawn without taking the interactions between the pigments into account. Nonetheless, there is considerable agreement between the spectral decomposition proposed by Remelli and co-workers and our results on the composition of the energy bands. For instance, the Chls B1(*a*), a1, and a2 contribute to a large extent to the main absorption band on the red side and there are minor contributions to 663 nm band by a1. The absorption of the Chls a4 and a5 peaks is near 675 nm. The Chl A3(*a*) is partly responsible for an absorption band peaking near 662–663 nm and Chl B3(*a*) contributes to the bands at 666 and 673 nm. Owing to several stronger excitonic couplings, it is more difficult to compare the Chl *b* region assignments. However, the blue-most Chl *b* is b2 and the other Chls *b* are more on the red side in both studies.

Energy transfer processes in the LHCII, both in monomeric and trimeric forms, have been studied extensively by various time-resolved techniques (e.g. Eads et al. 1989; Kwa et al. 1992; Bittner et al. 1994; Du et al. 1994; Palsson et al. 1994; Savikhin et al. 1994; Visser et al. 1996; Connelly et al. 1997; Kleima et al. 1997; Gradinaru et al. 1998; Agarwal et al. 2000). The "intramonomeric" *b*-*a*, *a*-*a*, and *b*-*b* transfers with time scales ranging between 150 fs and 10 ps have been identified. In two-color transient absorption experiments exciting the Chl *b* region around 650 nm, three different time scales for the Chl *b* to Chl *a* transfers have been distinguished ($\leq$ 200 fs, $\approx$600 fs, and 2–6 ps) (Visser et al. 1996; Connelly et al. 1997; Agarwal et al. 2000). Their contribution to the Chl *b* to Chl *a* transfers have been found to be around 40%, 40%, and 20%, respectively.

Transient absorption measurements have indicated that the Chl(s) *a* absorbing around 663 nm transfers to the low-energy ones (absorbing 679 nm), either directly or via the 670 nm pool with a time constant of 5 ± 1 ps. The 670 nm excitation is transferred to the low-energy Chls *a* in two phases (300 ± 50 fs and 12 ± 2 ps) and a fast equilibration (450 ± 50 fs) takes place within the main absorption band (675–680 nm) (Gradinaru et al. 1998). In a recent 3PEPS (three-pulse photon echo peak shift) experiment (Agarwal et al. 2000), two decay channels of lifetimes around 320 fs and 5 ps upon 670 nm excitation have also been found. Chl *b* to Chl *b* transfers in the 650 nm band have been observed for the first time in the same 3PEPS study and a biexponential transfer (with lifetimes 300 and 800 fs) between a "pair" of Chls *b* has been reported. These observations have also suggested that the slowest *b* to *a* transfer is linked with the strongly coupled Chls *b* involved in the biexponential *b*-*b* transfer and, in addition, these groups of molecules are associated with a Chl *b* to Chl *a* decay pathway of lifetime around 600 fs.

In view of the results we have presented above, it is necessary to evaluate the energy equilibration by taking the delocalized nature of the excited states into account. Therefore it is not entirely proper to talk in terms of the Förster rates (Förster 1965) between the pairs of molecules. However, in order to discuss that one can in principle understand quite well the pathways and the time scales for flow of excitation energy within the proposed assignment, we have provided a block diagram in Fig. 3. The rate constants for this diagram are estimated using the Förster mechanism as described elsewhere in detail (Özdemir 1997; Gradinaru et al. 1998). The lowest excited states of the isolated chlorophylls are used in estimating the rate constants.

It was already evidenced by several previous studies that the excitation transfer in the LHCII and CP29 complexes are compartmental to a large extent (Özdemir 1997; Gradinaru 1998; Simonetto et al. 1999; İseri et al. 2001). Compartment refers to a group of molecules that transfer to/equilibrate with each other very fast ($<$ 1 ps) but has significantly slower transfers (5 ps) with the rest of the molecules in the system. The compartments, defined by the assignments of this study, are shown in Fig. 3.

Excitation is extensively delocalized among the Chls *a* belonging to the same compartment. The electronic excited state structures presented in this work furthermore indicate that the delocalization of excitation is not only limited to the compartments. Inter-compartmental interactions cause further delocalization of excitation. It is clear that excitation will be fully equilibrated over the compartmental Chls *a* since there are several bi-directional pathways between them. One of the two non-compartmental Chls *a*, A6, also equilibrates with this core through A6-a3 interaction ($\approx$20 ps; not shown in Fig. 3). The other one, A7, is the only unidirectional Chl *a* and feeds the a4-a5 pair. Excitation equilibration among all these delocalized levels in the Chl *a* spectral region needs to be detailed with further simulations of

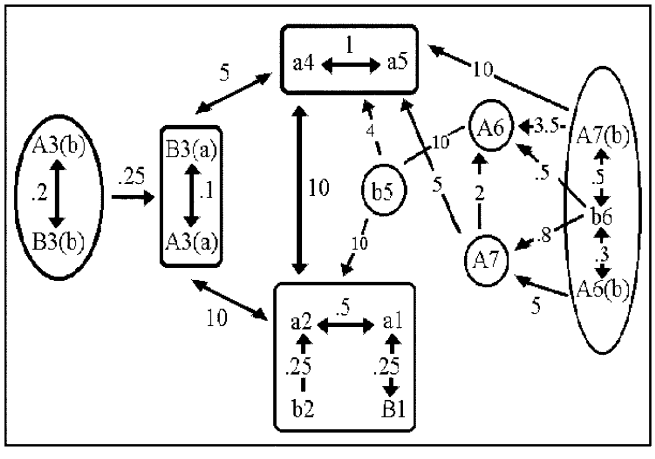

Fig. 3 Block diagram representation of the excitation pathways

energy transfer processes. Nevertheless, the time scales of the intra- (≤ 1 ps) and inter-compartmental (≈5–10 ps) transfers correlate well with the experimentally observed equilibration rates.

The fastest transfers from the 650 nm band flow out of the Chls *b*, B3, A3, and b2. The B3(*b*)-A3(*b*) pair is highly delocalized and equilibrates very rapidly (≤ 200 fs), but transfer of excitation from this Chl *b* pair to the Chl *a* pool is rather slow (≥10 ps, via B3-a2 interaction). Therefore the Chl *b* molecules B3 and A3 in the monomeric form are responsible for part of the ultrafast *b* to *a* transfer from the 650 nm band. Each, as a Chl *a* molecule, is weakly coupled with the rest of the Chl *a* molecules. The B3(*b*) to A3(*a*) and A3(*b*) to B3(*a*) transfers take about 250 fs. The other ultrafast Chl *b*, b2, on the other hand, transfers to a pool of strongly coupled Chls *a* via b2-a2 coupling (≈250 fs). In our model, the b5 molecule transfers to several Chl *a* molecules (a4, a5, A6, and B1) with transfer times ranging from 5 ps to 15 ps, yielding an overall de-excitation rate of around 2 ps. It is therefore likely to contribute both to the intermediate and slow *b* to *a* transfers. The remaining Chls *b*, A6, A7, and b6, constitute a strongly coupled group of molecules. In the compartment of these Chls *b* there are two subpicosecond transfers, b6-A6 (350 fs) and b6-A7 (500 fs). There is also b6-b5 equilibration, but this is several times slower (≥2 ps) and is not shown in the block diagram. Moreover, the *b* to *a* transfers which exit from this pool have two different time scales (subpico- and several picoseconds). The slow one proceeds mainly via A6(*b*) to A7(*a*) and A7(*b*) to A6(*a*) and a5 connections with the respective lifetimes of around 5 ps and 2.5 ps. The third Chl *b* of this pool, b6, de-excites by transferring both to A7(*a*) and A6(*a*). Each of these transfers is on the sub-picosecond scale, b6-A7 (800 fs) and b6-A6 (500 fs), yielding an overall de-excitation rate of around ≥300 fs. All these *b*-*b* and *b*-*a* transfer properties associated with the A7, A6, and b6 molecules are perfectly in agreement with the conclusions of the recent 3PEPS study of Agarwal et al. (2000). With these estimates of the rate constants, the contributions of the Chls *b* in the monomeric LHCII to the Chl *b*-Chl *a* transfers are around 40% (fast), 30% (intermediate), and 30% (slow).

LHCII in vivo is probably an aggregated form of the trimeric LHCII. Therefore, in addition to the intramonomeric transfers described above, one also expects intermonomeric and intertrimeric transfers. With the suggested orientations and the spectral assignments, the a4-a5 interaction between the adjacent monomers is the most favorite intermonomeric channel (estimated to have a Förster rate of around 15–20 ps).

Our choice on the identity of the molecule binding to site A7 has not been fully justified by site-directed mutagenesis. A7 has been suggested to be a pure Chl *b* binding site by Remelli et al. (1999). With the identity assignments of this mutagenesis work, however, the Chl *a*/*b* stochiometry (6.5*a*/5.5*b*) of the LHCII (7*a*/5*b*) is not satisfied. It has already been discussed that one of the sites A6 and A7 might be binding Chl *a* with a higher affinity (Remelli et al. 1999) and our choice has been to assign A7 as a mixed site with equal binding probability. Several remarks on this choice are necessary. Note that unless both A6 and A7 sites bind Chl *b* molecules it would not be possible to have a biexponential *b*-*b* transfer process with the transfer times observed (Agarwal et al. 2000) in the Chl *b* spectral region within the current identity assignments. Consequently, it would also not be possible to associate part of the slow *b* to *a* transfer with a group of strongly coupled Chls *b*. The dipole moment direction of the molecule binding to site A7 is very extreme: either almost in the molecular plane (0) or almost parallel to the C_3 symmetry axis (1). The orientation 0 gives a large positive LD and the orientation 1 yields a large negative LD signal. For this reason, it has been assigned to be in orientation 0 as a Chl *a* in the previous models (Trinkunas et al. 1997; Gradinaru et al. 1998). In this respect, it becomes rather difficult to explain the relative strengths of the LD signals and the values of the reduced LD in the Chl *b* and the Chl *a* bands if no Chl *a* character is associated with this molecule. One is referred to, for example, Gülen et al. (1997) for a more comprehensive discussion on this point.

Conclusions

We have assigned in this work the Q_y dipole moment orientations for all the chlorophylls in the major plant antenna, LHCII. We have assumed that the electronic excited states of the complex have been decided by the Chl-Chl and Chl-protein interactions and have modeled the coulombic interaction between a pair of Chls in the point dipole approximation and the Chl-protein interactions are treated as empirical fit parameters. A considerable part of the current information offered by structure determination, site-directed mutagenesis, and spectroscopy has been included in the modeling. The assignment proposed has been discussed to yield a satisfactory reproduction of all the prominent features of the polarized linear absorption spectra as well as the prominent spectral and temporal features of the energy transfer processes among the chlorophylls.

It is believed that, given the complexity of the system, the orientations and the spectral assignments obtained by relatively simple exciton calculations have been necessary, in order to provide a good point of departure for more detailed treatments of both the steady-state spectra (Krueger et al. 1998; Renger and May 2000) and the excitation kinetics (Leegwater et al. 1997; Renger and May 1998; Sumi 1999).

Acknowledgements We would like to thank to Dr. Werner Kühlbrandt for providing the data file containing the atomic coordinates of the LHCII structure and to Dr. Roberto Bassi for sharing some of the results from his laboratory with us prior to publication.

References

Agarwal R, Krueger BP, Scholes GD, Yang M, Yom J, Mets L, Fleming GR (2000) Ultrafast energy transfer in LHC-II revealed by three-pulse photon echo peak shift measurements. J Phys Chem B 104:2908–2918

Amerongen H van, Bolhuis BM van, Betts S, Mei D, Grondelle R van, Yocum CF, Dekker JP (1994) Polarized fluorescence and absorption of macroscopically aligned light harvesting complex II. Biophys J 67:837–847

Bassi R, Croce R, Cugini D, Sandona D (1999) Mutational analysis of a higher plant antenna protein provides identification of chromophores bound into multiple sites. Proc Natl Acad Sci USA 96:10056–10061

Bittner T, Wiederrecht KD, Irrgang K-D, Renger G, Wasielewski M (1994) Femtosecond transient absorption spectroscopy on the light-harvesting Chl *a*/*b* protein complex of photosystem II at room temperature and 12 K. Chem Phys 194:312–322

Boekema EJ, Roon H van, Calkoen F, Bassi R, Dekker JP (1999) Multiple types of association of photosystem II and its largest light-harvesting antenna in partially solubilized photosystem II membranes. Biochemistry 38:2233–2239

Connelly JP, Müller MG, Gatzen G, Mullineaux CW, Ruban AV, Horton P, Holzwarth AR (1997) Ultrafast spectroscopy of trimeric light-harvesting complex II from higher plants. J Phys Chem B 101:1902–1909

Du M, Xie X, Mets L, Fleming GR (1994) Direct observation of ultrafast energy-transfer processes in light-harvesting complex II. J Phys Chem 98:4736–4741

Eads DD, Castner EW, Alberte RS, Mets L (1989) Direct observation of energy transfer in a photosynthetic membrane: chlorophyll *b* to chlorophyll *a* transfer in LHC. J Phys Chem 93:8271–8276

Förster T (1965) Delocalization of excitation and excitation transfer. In: Sinanoğlu O (ed) Modern quantum chemistry, part II.b.1, Istanbul lectures, part III. Action of light and organic crystals. Academic Press, New York, pp 93–137

Fragata M, Norden B, Kurucsev T (1988) Linear dichroism (250–700 nm) of chlorophyll *a* and pheophytin *a* oriented in a lamellar phase of glycerylmonooctaonate/H_2O: characterization of electronic transitions. Photochem Photobiol 47:133–143

Giuffra E, Zucchelli G, Sandona D, Croce R, Cugini D, Garlaschi FM, Bassi R, Jennings RC (1997) Analysis of some optical properties of native and reconstituted photosystem II antenna complex CP29: pigment binding sites can be occupied by chlorophyll *a* or chlorophyll *b* and determine spectral forms. Biochemistry 36:12984–12993

Gradinaru CC, Özdemir S, Gülen D, Stokkum IHM van, Grondelle R van, Amerongen H van (1998) The flow of excitation energy in LHCII monomers: implications for the structural model of the major plant antenna. Biophys J 75:3064–3077

Gradinaru CC, Pascal A, Mourik F van, Robert B, Horton P, Grondelle R van, Amerongen H van (1999) Ultrafast evolution of the excited states in the minor chlorophyll *a*/*b* complex CP29 from green plants studied by energy-selective pump-probe spectroscopy. Biochemistry 37:1143–1149

Green BR, Kühlbrandt W (1995) Sequence conservation of light-harvesting and stress-response proteins in relation to the three-dimensional molecular structure of LHCII. Photosynth Res 44:139–148

Grondelle R van, Dekker JP, Gillbro T, Sundström V (1994) Energy transfer in photosynthesis. Biochim Biophys Acta 1187:1–65

Gülen D, Grondelle R van, Amerongen H van (1995) Structural information on light-harvesting complex II as obtained from exciton calculations and polarized spectroscopy. In: Mathis P (ed) Photosynthesis: from light to biosphere, vol I. Kluwer, Dordrecht, pp 335–338

Gülen D, Grondelle R van, Amerongen H van (1997) Structural information on the light-harvesting complex II of green plants that can be deciphered from polarized absorption characteristics. J Phys Chem B 101:7256–7261

Hemelrijk PW, Kwa SLS, Grondelle R van, Dekker JP (1992) Spectroscopic properties of LHCII, the main light-harvesting chlorophyll *a*/*b* protein complex from chloroplast membranes. Biochim Biophys Acta 1098:159–166

Hofmann E, Wrench P, Sharples FD, Hiller RG, Welte W, Diederichs K (1996) Structural basis of light-harvesting by carotenoids-peridinin-chlorophyll *a*-protein from *Amphidinium carterae*. Science 272:1788–1791

İseri E (1998) Electronic excited states and excitation transfer kinetics in the FMO protein complex of the photosynthetic bacterium *Prosthecochloris aestuarii* at low temperatures. MS Thesis, METU, Ankara, Turkey

İseri E, Gülen D (1999) Electronic excited states excitation transfer kinetics in the FMO protein complex of the photosynthetic bacterium *Prosthecochloris aestuarii* at low temperatures. Eur Biophys J 28:243–253

İseri E, Albayrak D, Gülen D (2001) Electronic excited states of the CP29 antenna complex of green plants. A model based on exciton calculations. J Biol Phys (in press)

Kleima FJ, Gradinaru CC, Calkoen F, Stokkum IHM van, Grondelle R van, Amerongen H van (1997) Energy transfer in LHC-II monomers at 77 K studied by subpicosecond transient absorption spectroscopy. Biochemistry 36:5262–5268

Kleima FJ, Hobe S, Calkoen F, Urbanus ML, Peterman EJG, Grondelle R van, Paulsen H, Amerongen H van (1999) Decreasing the chlorophyll *a*/*b* ratio in reconstituted LHCII: structural and functional consequences. Biochemistry 38:6587–6596

Kleima FJ, Hofmann E, Gobets B, Stokkum IHM van, Grondelle R van, Diederichs K, Amerongen H van (2000) Förster excitation energy transfer in peridinin-chlorophyll-*a*-protein. Biophys J 78:344–353

Krawzcyk S, Krupa Z, Maksymiec W (1992) Stark spectroscopy of chlorophylls and carotenoids in antenna pigment proteins LHC-II and CP-II. Biochim Biophys Acta 1143:273–281

Krueger BP, Scholes GD, Fleming GR (1998) Calculation of couplings and energy-transfer pathways between the pigments of LH2 by ab initio transition density cube method. J Phys Chem B 102:5378–5386

Kühlbrandt W, Wang DN, Fujiyoshi Y (1994) Atomic model of plant light-harvesting complex by electron crystallography. Nature 367:614–621

Kwa SLS, Amerongen H van, Lin S, Dekker JP, Grondelle R van, Struve WS (1992) Ultrafast energy transfer in LHC-II trimers from the Chl *a*/*b* light-harvesting antenna of photosystem II. Biochim Biophys Acta 1101:202–212

Leegwater AJ, Durrant RD, Klug DR (1997) Exciton equilibration induced by phonons: theory and its applications to PSII reaction centers. J Phys Chem B 101:7205–7210

Lokstein H, Leupold D, Voigt B, Nowak F, Ehlert J, Hoffman P, Garab G (1996) Nonlinear polarization spectroscopy in the frequency domain of light-harvesting complex II: absorption band structure and exciton dynamics. Biophys J 69:1536–1543

Louwe RJW, Vrieze J, Hoff AJ, Aartsma TJ (1997) Towards an integral interpretation of the optical steady-state spectra of the FMO complex of *Prosthecochloris aestuarii*. II. Exciton simulations. J Phys Chem B 101:11280–11287

Moog RS, Kuki A, Fayer MD, Boxer SG (1984) Excitation transport and trapping in a synthetic chlorophyllide substituted hemoglobin: orientation of the chlorophyll S_1 transition dipole. Biochemistry 23:1564–1571

Nussberger S, Dekker JP, Kühlbrandt W, Bolhuis BM, Grondelle R van, Amerongen H van (1994) Spectroscopic characterization of three different monomeric forms of the main chlorophyll *a*/*b* binding protein from chloroplast membranes. Biochemistry 33:14775–14783

Özdemir S (1997) Identification of several energy transfer pathways in the light-harvesting complex II of green plants using current structural and spectroscopic information. MS Thesis, METU, Ankara, Turkey

Palsson LO, Spangfort MD, Gulbinas V, Gillbro T (1994) Ultrafast chlorophyll *b*-chlorophyll *a* excitation transfer in the isolated light-harvesting complex, LHC, of green plants. FEBS Lett 339:134–138

Pascal A, Gradinaru CC, Wacker U, Peterman E, Calkoen F, Irrgang K-D, Horton P, Renger G, Grondelle R van, Robert B, Amerongen H van (1999) Spectroscopic characterization of the spinach Lhcb4 protein (CP29), a minor light-harvesting complex of photosystem II. Eur J Biochem 262:817–823

Pearlstein RM (1991) Theoretical interpretation of the antenna spectra. In: Scheer H (ed) The chlorophylls. CRC Press, Boca Raton, pp 1047–1078

Reddy NRS, Amerongen H van, Kwa SLS, Grondelle R van, Small GJ (1994) Low-energy exciton level structure and dynamics in light-harvesting complex II of green plants. J Phys Chem 98:4729–4935

Remelli R, Varotto C, Sandona D, Croce R, Bassi R (1999) Chlorophyll binding to monomeric light-harvesting complex. J Biol Chem 274:33510–33521

Renger T, May V (1998) Exciton motion in photosynthetic antenna systems: the FMO system. J Phys Chem A 102:4381–4391

Renger T, May V (2000) Simulations of frequency-domain spectra: structure-function relationships in photosynthetic pigment-protein complexes. Phys Rev Lett 84:5228–5231

Rogl H, Kühlbrandt W (1999) Mutant trimers of light-harvesting complex II exhibit altered pigment content and spectroscopic features. Biochemistry 38:16214–16222

Sauer K, Schmidt JRL, Schultz AJ (1966) Dimerization of chlorophyll *a*, chlorophyll *b*, and bacteriochlorophyll in solution. J Am Chem Soc 88:2681–2688

Savikhin S, Amerongen H van, Kwa SLS, Grondelle R van, Struve WS (1994) Low-temperature energy transfer in LHC-II trimers from the Chl *a*/*b* light-harvesting antenna of photosystem II. Biophys J 66:1597–1603

Simonetto R, Crimi M, Sandona D, Croce R, Cinque G, Breton J, Bassi R (1999) Orientation of chlorophyll transition dipole moments in the higher-plant light-harvesting complex CP29. Biochemistry 38:12974–12983

Sumi H (1999) Theory on rates of excitation-energy transfer between molecular aggregates through distributed transition dipoles with application to antenna system in bacterial photosynthesis. J Phys Chem B 103:252–260

Trinkunas G, Connelly JP, Müller MG, Valkunas L, Holzwarth A (1997) Model for excitation dynamics in the light-harvesting complex II from green plants. J Phys Chem B 101:7313–7320

Visser HM, Kleima FJ, Stokkum IHM van, Grondelle R van, Amerongen H van (1996) Probing many energy-transfer processes in the photosynthetic light-harvesting complex II at 77 K using energy selective sub-picosecond transient absorption spectroscopy. Chem Phys 210:297–312. Erratum: (1997) Chem Phys 215:299

Vulto SIE, Baat MA de, Louwe RJW, Permentier HP, Neef T, Miller M, Amerongen H van, Aartsma, TJ (1998) Exciton simulations of optical spectra of the FMO complex from the green sulfur bacterium *Chlorobium tepidum* at 6 K. J Phys Chem B 102:9577–9582

Zandvoort MAMJ van, Wrobel D, Lettinga P, Ginkel G van, Levine YK (1995) The orientation of the transition dipole moments of chlorophyll *a* and pheophytin in their molecular frame. Photochem Photobiol 62:299–308

Zucchelli G, Dainese P, Jennings RC, Breton J, Garlaschi FM, Bassi R (1994) Gaussian decomposition of absorption and linear dichroism spectra of outer antenna complexes of photosystem II. Biochemistry 33:8982–8990